Available online at www.sciencedirect.com
ScienceDirect
Journal of Sound and Vibration 302 (2007) 361–378
JOURNAL OF SOUND AND VIBRATION
www.elsevier.com/locate/jsvi

Dynamic model including piping acoustics of a centrifugal compression system

Jan van Helvoirt[a,b,*], Bram de Jager[a]

[a]Control Systems Technology Group, Department of Mechanical Engineering, Technische Universiteit Eindhoven, P.O. Box 513, 5600 MB Eindhoven, The Netherlands
[b]Flow and Structural Dynamics Group, Division Industrial Modeling and Control, TNO Science and Industry, P.O. Box 126, 2600 AB Delft, The Netherlands

Received 6 September 2006; received in revised form 28 November 2006; accepted 4 December 2006
Available online 16 January 2007

Abstract

This paper deals with low-frequency pulsation phenomena in full-scale centrifugal compression systems associated with compressor surge. The Greitzer lumped parameter model is applied to describe the dynamic behavior of an industrial compressor test rig and experimental evidence is provided for the presence of acoustic pulsations in the compression system under study. It is argued that these acoustic phenomena are common for full-scale compression systems where pipe system dynamics have a significant influence on the overall system behavior.

The main objective of this paper is to extend the basic compressor model in order to include the relevant pipe system dynamics. For this purpose a pipeline model is proposed, based on previous developments for fluid transmission lines. The connection of this model to the lumped parameter model is accomplished via the selection of appropriate boundary conditions.

Validation results will be presented, showing a good agreement between simulation and measurement data. The results indicate that the damping of piping transients depends on the nominal, time-varying pressure and flow velocity. Therefore, model parameters are made dependent on the momentary pressure and a switching nonlinearity is introduced into the model to vary the acoustic damping as a function of flow velocity.

These modifications have limited success and the results indicate that a more sophisticated model is required to fully describe all (nonlinear) acoustic effects. However, the very good qualitative results show that the model adequately combines compressor and pipe system dynamics. Therefore, the proposed model forms a step forward in the analysis and modeling of surge in full-scale centrifugal compression systems and opens the path for further developments in this field.

1. Introduction

In this paper, we address low-frequency pulsation phenomena in large industrial compression systems associated with compressor surge. Surge is an unstable operating mode of a compression system that occurs at low mass flows. The instability is characterized by large limit-cycle oscillations in compressor flow and

*Corresponding author. Department of Mechanical Engineering, Control Systems Technology Group, Technische Universiteit Eindhoven, P.O. Box 513, 5600 MB Eindhoven, The Netherlands. Tel.: +31 40 2472811; fax: +31 40 2461418.
E-mail address: j.v.helvoirt@tue.nl (J. van Helvoirt).

0022-460X/$ - see front matter
doi:10.1016/j.jsv.2006.12.003

Nomenclature

A	area (m^2)
c	speed of sound (m/s)
F	frequency dependent friction factor
G, H, K	transfer functions
L	duct length (m)
$\dot{m}$	mass flow (kg/s)
N	rotor speed (rev/min)
p	pressure ($kg/m\,s^2$)
q	volume flow (m^3/s)
r	pipe radius (m)
R	pipe resistance ($kg/m^3\,s$)
Re	Reynolds number (dimensionless)
s	Laplace variable
t	time (s)
T	temperature (K)
u	flow velocity (m/s)
V	volume (m^3)
x	position (m)
y	valve opening (dimensionless)
z	specific acoustic impedance ($kg/m^2\,s$)
Z	acoustic impedance ($kg/m^4\,s$)

Greek

κ	numerical constant (dimensionless)
ρ	density (kg/m^3)
μ	dynamic viscosity (kg/m s)
τ	time constant (s)
Φ	characteristic variable (dimensionless)
Ψ	characteristic variable (dimensionless)
ω	angular frequency (rad/s)

Subscripts

0	nominal, mean value
1	suction side
2	discharge side
$+$	positive, left going
$-$	negative, right going
c	compressor
d, n, l	cut-off frequencies
i, j	general indices
p	pipe
t	throttle
v	viscous
w	wall

Superscripts

$\sim$	acoustic perturbation

pressure rise. Surge not only reduces machine performance but the large thermal and mechanical loads can also damage the compression system.

Modeling of compression system dynamics has received significant attention over the years and this has lead to a better understanding of the unstable phenomena and the underlying physics. Extensive surveys of this field are given in Refs. [1–3]. However, most work in this field was done for axial compressors and fewer results are available on centrifugal compressors. This holds in particular for surge in large, high-power centrifugal compressors, typically found in the oil and gas and process industry.

One of the first nonlinear models of transient compression system behavior was proposed in Ref. [4]. This model exploited the analogy between surge oscillations and a Helmholtz resonator, an idea first suggested in the linearized analysis of Ref. [5]. Although developed for axial compressors, the authors of Ref. [6] showed that this nonlinear model was also applicable to centrifugal compressors. To this day, it is the most widely used dynamic model in the field. Many modifications and extensions were suggested, for example in Refs. [7–9], but the basic principle of the so-called *Greitzer model* remained unaltered.

It is important to note that the Greitzer model is a so-called lumped parameter model. Together with various other assumptions, the lumping approach results in a relatively simple and low-order model for the dynamic behavior of a compression system. However, lumped parameter models are not suitable for describing phenomena associated with the distributed nature of fluid flows like acoustic waves and flow pulsations. In particular for large, industrial systems these phenomena can have a significant influence on the dynamic behavior of the entire compression system.

In full-scale centrifugal compression systems the compressor outlet is usually connected to a long discharge line rather than to a large volume like a vessel. The strong influence of piping acoustics on the transient response and flow stability of centrifugal compressors was addressed in Ref. [10]. The main conclusion from this work was that surge is a system instability whose onset is determined by system acoustic damping and whose frequency is determined largely by the attached piping.

The effect of shock waves—a violent acoustic phenomenon—that occur during the first milliseconds of a surge cycle on the dynamic behavior of high-speed axial compressors was addressed in Ref. [11]. In Ref. [12], the authors briefly mentioned the similarity with acoustic ducts in their discussion on the distributed character of compressible flows. Furthermore, the authors of Ref. [13] investigated active and passive control for systems with various inlet and discharge piping configurations. However, their study on piping system dynamics was rather limited since they only included the piping capacitance in a modified Greitzer lumped parameter model.

The study of flow pulsations in pipelines has become common practice in industry, for a great deal originating from the pulsation problems arising from the use of reciprocating compressors, see for example Refs. [14–16]. Research on acoustics, fluid–structure interactions and transients in fluid transmission lines is a mature field as indicated by the many available publications and textbooks like Refs. [17–21]. Unfortunately, hardly any quantitative results are available from literature on the coupling between piping acoustics and the dynamic behavior of axial and centrifugal compressors.

1.1. Scope of the paper

In this paper, we will address the influence of the piping system on the transient behavior of a full-scale centrifugal compression system. We will discuss the application of the Greitzer lumped parameter model to model an industrial compressor test rig. Secondly, we will provide experimental evidence for the presence of acoustic pulsations in the compression system under study. The discussion of the experimental setup and the dynamic model for this system form the starting point for the subsequent sections.

The main objective of this paper is to present an extension of the basic compressor model that accounts for the relevant piping system dynamics. Hence, we proceed with a brief introduction of acoustic terminology and the underlying physics, after which we propose a model structure for compressor piping systems that is based on previous developments for fluid transmission lines. Then we discuss how this model can be connected to the lumped parameter model via the choice of appropriate boundary conditions and model parameters. Simulation results will be presented to show that the combined model provides a more detailed description of the dynamic behavior of the entire centrifugal compression system. Finally, we summarize the main conclusions from this work and we formulate directions for further research.

2. Centrifugal compression system

All experiments described in this paper were conducted on a full-scale centrifugal compression system. In this section, we introduce the main components and instrumentation of the installation. Furthermore, we introduce the equations for the nonlinear lumped parameter model, similar to the original Greitzer model. We validate the model by comparing simulation results with data from actual surge measurements. These results are also used to illustrate the need for a model extension to account for piping system dynamics in order to improve the agreement between simulations and measured data.

2.1. Experimental setup

The system under study is a single-stage, centrifugal compressor rig that is normally used to test industrial compressors for the oil and gas industry. The whole installation is schematized in Fig. 1. The compressor is driven by an 1 MW electric motor and typical rotational speeds of the compressor lie between 14,000 and 21,000 rev/min. The impeller that is mounted on the shaft has 17 blades and an outer diameter of 0.3 m.

The compressor is connected to atmosphere via long suction and discharge piping. The discharge piping contains a measurement section with a flow straightener, and an orifice flow meter with a diameter ratio of 0.392. Accuracy of the mass flow measurements is ±3%, according to Ref. [22]. Throttling of the compressor

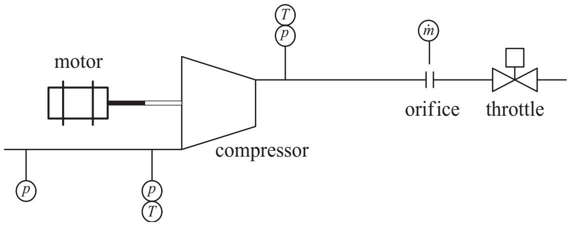

Fig. 1. Scheme of compressor test rig.

Table 1
Parameters of the compressor test rig

Parameter	Value	Unit
Compressor duct length L_c	10.6	m
Compressor duct area A_c	0.0255	m^2
Suction volume V_1	3.57	m^3
Suction piping length L_1	29.6	m
Discharge volume V_2	9.82	m^3
Discharge piping length L_2	41.9	m

is done by means of a large butterfly valve located at the end of the discharge line. The overall dimensions of the installation, relevant for the dynamic model, are summarized in Table 1.

The compression installation is equipped with numerous temperature probes and static pressure transducers to determine the steady-state performance of the compressor. Additional dynamic total pressure probes were installed in the suction and discharge pipes to measure the pressure rise fluctuations during experiments, see also Fig. 1.

The 3 suction side and 2 discharge side probes are located approximately 1 m upstream and downstream of the compressor, oriented along the circumference at 90° and 180° relative angles, respectively. Accuracy of the probes is ±5%, with respect to a full range of 0–3.5 bar differential and ambient pressure as reference. Suction and discharge pressures are obtained by averaging the readings from the individual probes at the corresponding location.

For data-acquisition a stackable measurement system with a total of 16 input channels, anti-aliasing filters and A/D convertors was used. All signals were measured at a sampling rate of 256 Hz.

2.2. Compressor model

In order to describe the dynamic behavior of the centrifugal compression system we used a lumped parameter model, analogous to Ref. [4]. The Greitzer model, as mentioned one of the first models capable of describing compressor transients, is graphically depicted in Fig. 2.

The main assumptions for the Greitzer lumped parameter model are

(1) plenum diameter is much larger than that of the compressor duct;
(2) inlet Mach number is low;
(3) small pressure rises compared to ambient pressure;
(4) surge frequency is below the duct's cut-off frequency;
(5) plenum dimensions are smaller than the acoustic wavelengths associated with surge;
(6) processes in the plenum are isentropic.

The first assumption implies that the kinetic energy of the oscillations is associated with motion of the fluid in the compressor duct, while the potential energy is associated with compression of the fluid inside the plenum. The second and third assumption indicate that it is reasonable to consider the fluid flowing through the duct to

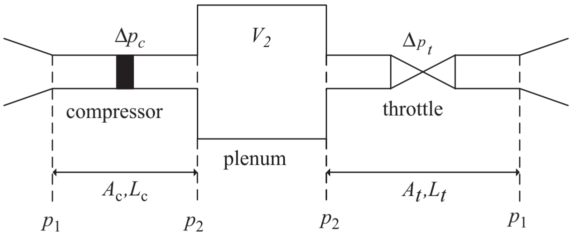

Fig. 2. Schematic representation of the Greitzer model.

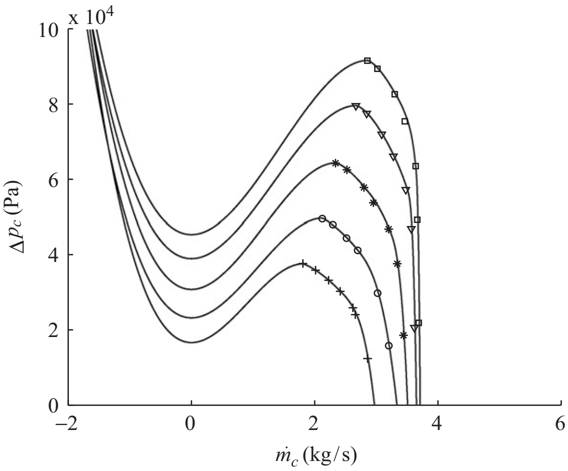

Fig. 3. Measured operating points and approximated compressor map. + 13,783 rev/min; ○ 15,723 rev/min; ∗ 17,636 rev/min; ▽ 19,512 rev/min; □ 20,855 rev/min.

be incompressible, with the density taken equal to the ambient value. Furthermore, the fourth assumption indicates that the flow in the compression system can be considered to be one-dimensional.

From the first and fifth assumption it follows that fluid velocity is negligible and static pressure is uniformly distributed inside the plenum. We will come back to this assumption in detail later on. Finally, the last assumption implies that viscous effects can be neglected.

The Greitzer model is based on the principles of mass and momentum conservation. Applying these principles with the above assumptions yields

$$\frac{L_c}{A_c}\frac{\mathrm{d}\dot{m}_c}{\mathrm{d}t} = \Delta p_c(\dot{m}_c, N) - \Delta p, \tag{1}$$

$$\frac{V_2}{c_2^2}\frac{\mathrm{d}p_2}{\mathrm{d}t} = \dot{m}_c - \dot{m}_t(\Delta p, y_t) \tag{2}$$

with $\Delta p = p_2 - p_1$. The forcing term $\Delta p_c(\dot{m}_c, N)$ denotes the pressure rise over the compressor as function of compressor mass flow and rotational speed. This so-called compressor characteristic is determined by fitting a polynomial or spline function through measured and calculated operating points, see for example Refs. [9,23]. The result for the investigated compressor is shown in Fig. 3.

We point out that in the original model a second impulse balance is derived for the throttle duct. However, the dynamics in the throttle duct can be neglected when $L_t/A_t \ll L_c/A_c$, which is usually the case, see for example Refs. [7,23].

When inertial effects in the throttle duct are neglected, the throttle mass flow $\dot{m}_t$ is no longer a state in the model. Instead, it can be described by a static mapping from Δp to $\dot{m}_t$ or in other words, by a static throttle characteristic. An expression for $\dot{m}_t(\Delta p, y_t)$ was obtained from Ref. [24], see also Fig. 7.

Furthermore, the original Greitzer model contains a dynamic equation that accounts for the deviations from quasi-steady behavior during the development of rotating stall. Since we want to study the pure surge case, this relaxation equation is omitted from the model.

Finally, it is common practice to reformulate the differential equations in non-dimensional form. However, to simplify the connection of the acoustic pipeline model, we will use the full-dimensional form throughout this paper.

2.3. Model validation

We evaluated the developed compressor model by comparing simulation results with data from actual surge measurements. At the start of each measurement the compressor was brought into surge by closing the throttle valve, after which the dynamic pressure oscillations were measured for 128 s. The temperature and pressure data were also used to initialize the simulation model.

To improve the match between measurement and simulation we selected the compressor duct length, the valley point of the compressor characteristic, and the throttle valve opening as tuning parameters. We used an optimization and search routine to determine which valley point and throttle opening resulted in the best match with the measurement. This procedure was carried out for different values of L_c and we selected the smallest compressor duct length that gave satisfactory results. A better way to identify L_c is described in Refs. [25,26] but for the investigated setup no transient data is available yet.

The final results for two particular measurements are shown in Figs. 4 and 5, both revealing a good agreement between the measured pressure oscillations and the outcome of the tuned simulation model. However, we point out that the power spectral densities of the measurements are higher than those of the simulation results in between the harmonic peaks of the surge oscillation. This is caused by the significant flow noise (e.g. turbulence) and some measurement noise that are present in the experimental system, which are not included in the simulation model.

More importantly, zooming in on one surge cycle reveals some differences between the measured and simulated time-series as can be seen in Fig. 6. In the first place, we remark that the measured pressure appears to increase faster than the simulated pressure after reaching its minimum value. A possible explanation for this difference is the influence of rotor speed variations during surge. Qualitative observations during the surge experiments indicated that the compressor slows down during the negative flow phase of each surge cycle. However, no quantitative data of compressor speed and drive torque is available to investigate the effect of rotor speed variations in more detail, for example by including rotor dynamics in the Greitzer model as proposed in Ref. [7].

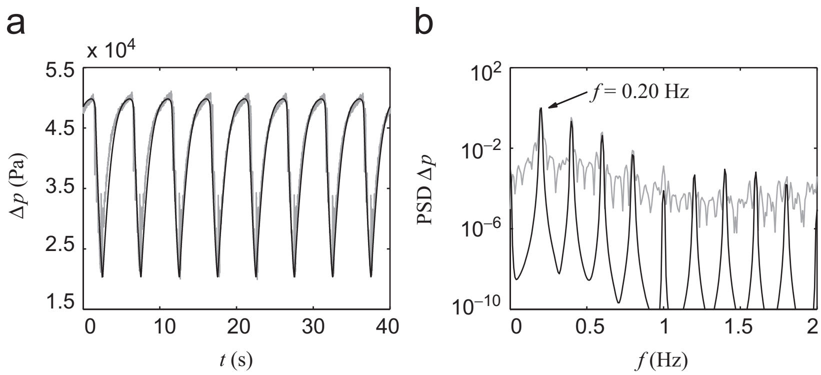

Fig. 4. Pressure measurement (gray) and simulation result of the tuned Greitzer model (black) during surge at $N = 15,723$ rev/min: (a) time-series and (b) power spectral density.

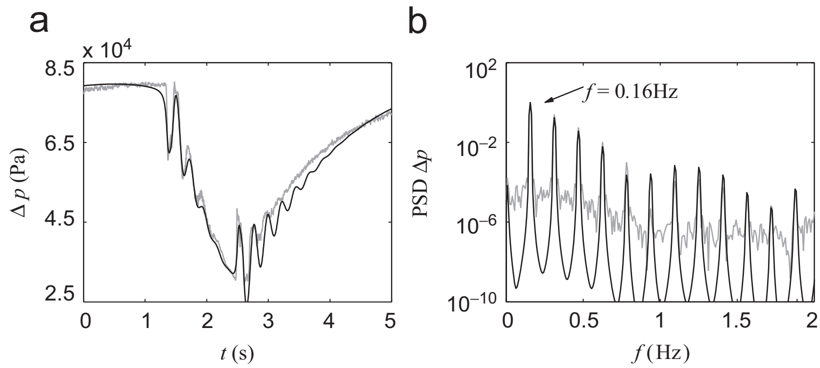

Fig. 5. Pressure measurement (gray) and simulation result of the tuned Greitzer model (black) during surge at $N = 19,512\,\mathrm{rev/min}$: (a) time-series and (b) power spectral density.

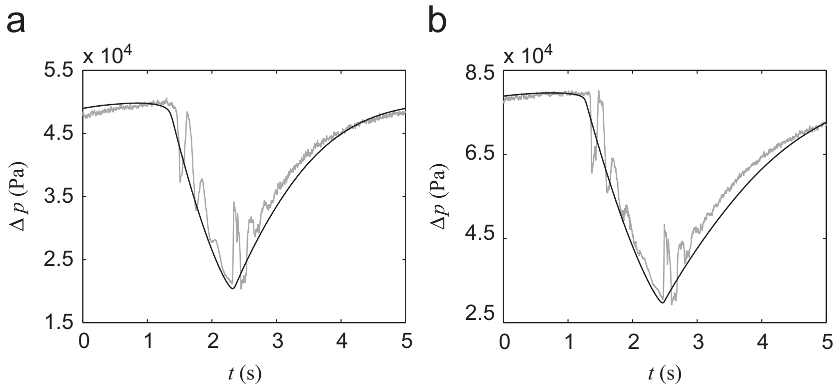

Fig. 6. Close-up of pressure measurements (gray) and simulation results of the tuned Greitzer model (black) at two rotational speeds: (a) $N = 15,723\,\mathrm{rev/min}$ and (b) $N = 19,512\,\mathrm{rev/min}$.

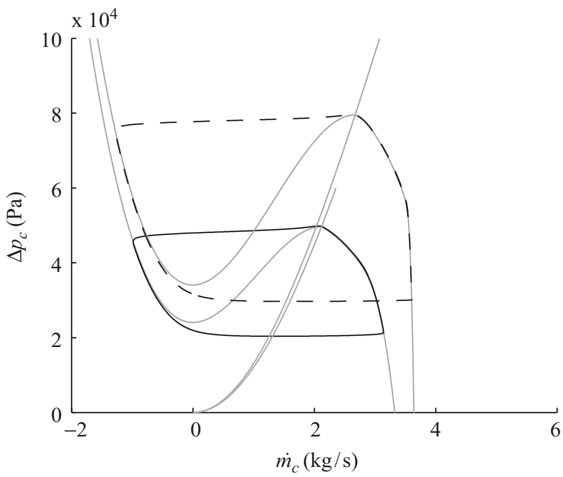

Fig. 7. Simulated limit cycles during surge at $N = 15,723\,\mathrm{rev/min}$ (solid line) and $N = 19,512\,\mathrm{rev/min}$ (dashed line).

Secondly, in Fig. 6 we observe various rapid pressure transients of decreasing amplitude in the measured signals that are not captured by the simulation model. From the simulated surge limit cycle in Fig. 7 we can see that the pressure transients occur after each flow reversal.

Close inspection of the rapid transients reveals a resemblance of the signal shape with that of a pressure response in a fluid transmission line subjected to a stepwise change in flow, see for example Ref. [17]. Furthermore, when a correction ($c \pm u$) is applied for the speed of sound and mean flow velocity, the duration of the fast transients appears to be almost independent (relative difference $<1.5\%$) of compressor rotational speed and surge frequency. Finally, transients as observed in Fig. 6 were not present in measurements on a similar full-scale test rig with a much shorter discharge line of 1.45 m instead of 41.9 m, see Ref. [26].

Based on the above findings we conclude that the damped pressure oscillations, occurring after each flow reversal, are the result of acoustic waves traveling back and forth in the discharge piping. Therefore, we will now discuss how the lumped parameter model can be extended to take into account the acoustic phenomena in the piping system.

3. Piping system acoustics

The study of flow and pulsations in piping systems is a field on its own with applications ranging from process plants to musical instruments. One of the many textbooks on flow–structure interactions is Ref. [20]. Over the years, high-order finite element, boundary element and finite difference methods have been developed to solve the governing equations. An attractive simplification follows from the fact that the wave equation is linear and hence that it is usually appropriate to limit the analysis to that of harmonic perturbations. In that case, a linear frequency domain model is sufficient for describing the sound propagation and this approach is extensively used in the literature, see for example Refs. [19,27]. However, coupling these linear system descriptions to a, in many cases nonlinear, source description is not always straightforward as discussed in Ref. [28].

Waves propagate through a piping system with finite speed as we discussed in the previous section. To cover this aspect of acoustics, so-called transmission line models or derivatives have been proposed in literature. Originating from the field of power systems, this type of model is used in many fields of applications like hydraulics [17,18], communication networks [29], and music synthesis [30].

Of equal importance as the wave propagation through the pipes, is the behavior of the fluid at the pipe boundaries. To completely describe the piping system acoustics, the wave propagation model must be augmented with proper boundary conditions that describe the, possibly nonlinear, coupling between the pipe and adjacent system components or the environment.

In this section, we will propose an acoustic model for the discharge piping to account for the acoustic pressure fluctuations behind the compressor. After discussing the wave propagation model we address the selection of appropriate boundary conditions. These boundary conditions will enable the coupling of the pipeline model to the Greitzer lumped parameter model for the compression system under study.

3.1. Dynamic model for piping system

The model for the compressor discharge piping is based on the pipeline model presented in Ref. [31]. This model was derived by using the method of characteristics and the authors showed that it captures the essential dynamics of a finite wave propagation speed and distributed frequency-dependent friction. Benefits of the model are its robustness, accuracy, computational efficiency and its straightforward interface towards connected systems or the environment.

The main assumptions for the pipeline model are

(1) acoustic perturbations of p, T, ρ, c are small compared to their undisturbed values;
(2) disturbances propagate isentropically along the transmission line;
(3) thermal effects are negligible;
(4) surge frequency is below the duct's cut-off frequency.

The first assumption implies that a linear model is sufficient to describe the propagation of acoustic waves. The second assumption allows the introduction of the isentropic speed of sound into the state equation. The third assumption implies that the energy equation can be ignored. Finally, the fourth assumption indicates that the flow in the pipeline can be considered to be one-dimensional. In other words, only planar acoustic waves will propagate through the pipeline. See the review paper [18] for an extensive overview of the various assumptions used in transmission line modeling.

As mentioned, the pipeline model is based on the method of characteristics that uses the fact that pressure and flow are related to each other by the following characteristic variables:

$$\Phi(x,t) = p(x,t) + Z_0 q(x,t), \quad \Psi(x,t) = p(x,t) - Z_0 q(x,t), \tag{3}$$

where Φ and Ψ are associated with right and left traveling waves, respectively. Here, the right traveling wave is defined as moving from the compressor outlet ($x = 0$) to the end of the pipe ($x = L$). The parameter $Z_0 = \rho_0 c_0 / A$ represents the acoustic impedance of a filled pipe with cross-sectional area A.

The boundary conditions at the ends of the line are described by adjacent components where the flow is typically a function of the pressure. Using Eq. (3), we get the following set of general equations that has to be solved at the left end ($x = 0$) of the line

$$q_i(t) = f(p_i(t)), \tag{4}$$

$$p_i(t) = Z_0 q_i(t) + \Psi_i(t) \tag{5}$$

and, similarly, for the right end ($x = L$) of the line

$$q_j(t) = f(p_j(t)), \tag{6}$$

$$p_j(t) = Z_0 q_j(t) + \Phi_j(t), \tag{7}$$

where $q = uA$ represents the volume flow in the line. The general indices i,j are used to denote the pipeline boundaries. Note that we have used the convention that flows entering the line are positive.

According to Ref. [31], in the frequency domain a transmission line can be described by the following equation:

$$\begin{bmatrix} \cosh\left(\tau\sqrt{F(s)}\right) & -\dfrac{1}{Z_0\sqrt{F(s)}}\sinh\left(\tau\sqrt{F(s)}\right) \\ -Z_0\sqrt{F(s)}\sinh\left(\tau\sqrt{F(s)}\right) & \cosh\left(\tau\sqrt{F(s)}\right) \end{bmatrix} \begin{bmatrix} Q_i(s) \\ P_i(s) \end{bmatrix} = \begin{bmatrix} -Q_j(s) \\ P_j(s) \end{bmatrix}, \tag{8}$$

where $F(s)$ is a frequency-dependent friction factor. The time delay $\tau = L/c_0$ corresponds to the time needed for a wave to travel through the pipe.

In the case of a uniformly distributed resistance, $F(s)$ is given by

$$F(s) = \frac{R}{Z_0 \tau s} + 1, \tag{9}$$

where R represents the total resistance in the line. In the case of frequency dependent friction, the expression for $F(s)$ is much more complicated [31].

By using Eqs. (4)–(7) we can rewrite Eq. (8), yielding

$$\Psi_i(s) = \mathrm{e}^{-\tau s\sqrt{F(s)}}\left(P_j(s) + Z_0\sqrt{F(s)}Q_j(s)\right) + Z_0\left(\sqrt{F(s)} - 1\right)Q_i(s), \tag{10}$$

$$\Phi_j(s) = \mathrm{e}^{-\tau s\sqrt{F(s)}}\left(P_i(s) + Z_0\sqrt{F(s)}Q_i(s)\right) + Z_0\left(\sqrt{F(s)} - 1\right)Q_j(s). \tag{11}$$

In order to enable inverse transformation of the above model into the time domain, some simplifications are required. For that purpose the authors of Ref. [31] used the block diagram for the derived pipeline model as shown in Fig. 8.

The frequency region of interest lies around $1/2\tau$, corresponding to the time period in which a wave can travel through the entire pipeline and back. By approximating the asymptotes of Eqs. (10) and (11) and matching the steady-state pressure drop in the line, the following rational transfer functions were obtained:

$$H(s) = \frac{R}{\kappa\tau s + 1}, \tag{12}$$

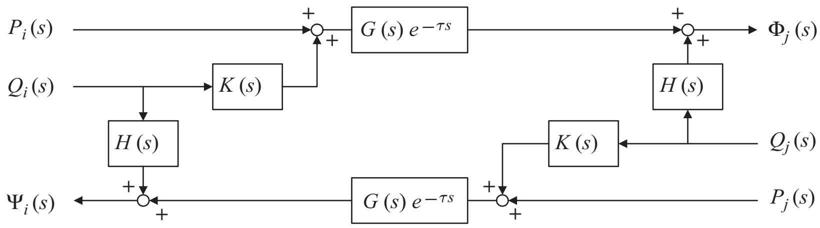

Fig. 8. Acoustic model for discharge line.

$$K(s) = Z_0, \tag{13}$$

$$G(s) = \frac{s/\omega_n + 1}{(s/\omega_l + 1)(s/\omega_d + 1)}, \tag{14}$$

where $\omega_d = 1/\kappa\tau$ and $\omega_n = \omega_d \mathrm{e}^{R/2Z_0}$, see Ref. [31]. A suitable value κ was found by numerical experiments, yielding $\kappa = 1.25$. The value of ω_l can be used to tune the low-pass filter part of Eq. (14) in order to get the correct attenuation at a particular frequency, for example to match the damping of a higher harmonic. This low-pass filter has been introduced to circumvent the use of the complex and unpractical expression for $F(s)$ in the case of frequency-dependent friction. Modeling the acoustic damping due to the friction in the system will be discussed in detail later on.

We point out that the introduced rational transfer functions are only a low-order approximation of the irrational representation of Eq. (8). Higher-order approximations might improve the accuracy of the model at the cost of increased complexity. The focus of this paper is to include those acoustic effects that have the largest impact on the overall system behavior during surge and hence a low-order approximation is considered to be sufficient, see also Ref. [32]. Higher-order approximation techniques for the irrational transmission line model are discussed in for example Ref. [33].

To summarize, a good approximation of a discharge pipeline with distributed, frequency-dependent resistance is defined by Fig. 8 and Eqs. (12)–(14). We can obtain a time-domain solution $(q_i(t), p_i(t), q_j(t), p_j(t))$ by choosing an appropriate numerical implementation. For example, we can use inverse Laplace transformation of inputs and outputs or convert the filters into difference equations via a bilinear transformation. These and other techniques are readily available in modern computational software packages.

3.2. Piping boundary conditions

Finally, the acoustic model for the discharge piping must be connected to the dynamic model of the compression system by selecting appropriate boundary conditions at each end of the pipeline, see also Ref. [28]. Generally speaking, boundary conditions are associated with a change of the acoustic impedance. At any point in the system where the acoustic impedance changes, an incident wave will be (partially) reflected. This property will be used to select boundary conditions that enable us to couple the acoustic model of the discharge piping to the lumped parameter model, given by Eqs. (1) and (2).

For that purpose it is convenient to use the simplified two-port representation of the Greitzer model given in Fig. 9. From this figure, we see that the input $q_i(t)$ for the line model can be obtained directly from the impulse balance of the adjacent section of the compressor model. More specifically, $q_i(t) = q_c(t)$ is calculated by dividing $\dot{m}_c(t)$, provided by Eq. (1), with ρ_2. Note that in this notation the required transformation between time and frequency domain is omitted. The line input $p_i(t)$ at the left boundary is calculated via Eq. (5). Note that this pressure represents the pressure downstream of the compressor, so now $\Delta p(t) = p_i(t) - p_1$ with $p_i(t) = p_c(t)$ has to be used in Eq. (1).

Selecting a second prescribed flow boundary condition at the other end of the line would only allow the trivial solution $q_i(t) = q_j(t)$, $p_i(t) = p_j(t)$. Therefore, the prescribed flow boundary at the entrance of the discharge line model dictates a prescribed pressure boundary condition at the other end of the line. A suitable

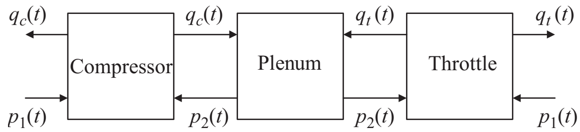

Fig. 9. Two-port representation of the Greitzer model.

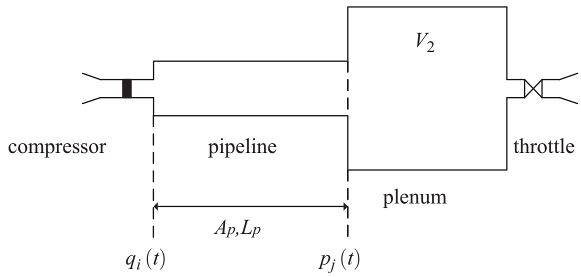

Fig. 10. Schematic representation of a pipeline-plenum boundary condition.

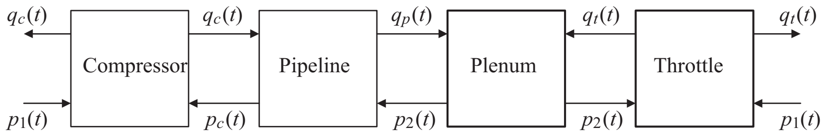

Fig. 11. Two-port representation of the combined Greitzer-pipeline model.

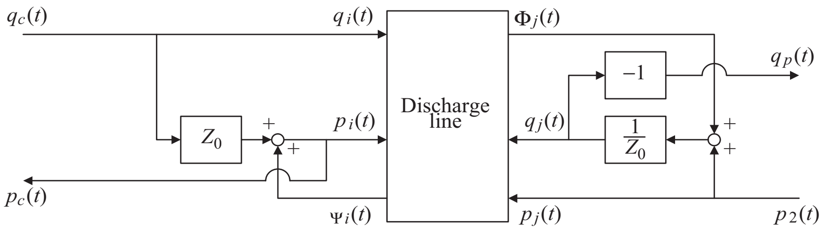

Fig. 12. Two-port representation of the pipeline model boundary conditions.

boundary of this kind is for example a point where the pipeline is connected to a vessel or a pipe with a larger diameter, i.e. a plenum volume. Such a boundary is schematically depicted in Fig. 10.

The prescribed pressure for such a boundary condition is provided by the plenum mass balance, yielding $p_j(t) = p_2(t)$ with $p_2(t)$ from Eq. (2). The flow variable $q_j(t) = q_p(t)$ at the right boundary is then calculated via Eq. (7) and the corresponding mass flow $\dot{m}_p(t)$ $(= q_p(t)\rho_2)$ replaces $\dot{m}_c(t)$ in Eq. (2). Note the sign convention in Eq. (8) that all flows entering the line are positive.

When physically plausible, another option to obtain a non-trivial system is to place a flow restriction with a known flow–pressure relation (e.g. a throttle) between the end of the line and a constant pressure reservoir. In that case a plenum volume is not needed and Eqs. (6) and (7) can be combined to provide the variables $q_j(t)$ and $p_j(t)$ at the line boundary.

Based on numerical experiments and practical experience we neglect the effect of acoustic perturbations on throttle mass flow, i.e. acoustic effects behind a plenum volume or pipe with a sufficiently large diameter do not need to be modeled. Hence, in our case the compressor and plenum volume from Fig. 2 provide the boundary conditions for the acoustic model of the discharge line. A two-port representation of the proposed coupling between the Greitzer model and the discharge line model is given in Fig. 11 while Fig. 12 shows the pipeline model boundary conditions in more detail. In the next section, we will address the implementation of the developed model and we will discuss the simulation results that were obtained.

4. Numerical results

The numerical implementation of the proposed pipeline model was done in accordance with Fig. 11. Details of the pipeline model and the coupling with the original Greitzer model are shown in Figs. 8 and 12. In order to carry out simulations for the centrifugal compression system under study, the parameters for the pipeline model must be set to appropriate values.

An important parameters that determines the damping of acoustic transients is the resistance or friction coefficient R. For turbulent flows the viscous friction coefficient R is usually estimated by using Blasius' empirical law [34]

$$R = 0.1582 Re^{3/4} \frac{\mu}{D^2}, \tag{15}$$

where $Re = \rho_0 u_0 D/\mu$ is the Reynolds number and μ denotes the dynamic viscosity of the medium. With the above formula we calculated an average value of R by using the various flow conditions that were encountered in the compression system under study, yielding $\bar{R} \approx 0.674$.

The cut-off frequency ω_l of the low-pass filter in $G(s)$ was initially set to $2/\tau = 2c_0/L_p$ during simulations, neglecting the influence of the mean flow velocity u_0. The influence of the parameter ω_l on the acoustic damping properties of the model will be discussed in more detail below. Values for the density and speed of sound are obtained from gas property tables in Ref. [35], using pressure and temperature measurements at the start of an experiment.

In order to define the time delays and the acoustic impedance, also values for L_p and A_p are needed. Initial simulations showed that the dominant acoustic effects are captured correctly when the pipeline-plenum boundary is placed at the first diameter change of the discharge piping, see also Fig. 13. A tuning procedure was followed to determine the precise pipeline length L_p and plenum volume V_2, similar to the method that we used for the original Greitzer model of the test rig. The resulting simulation parameters are summarized in Table 2. We remark that all tuning procedures were carried out for one particular set of measurement data.

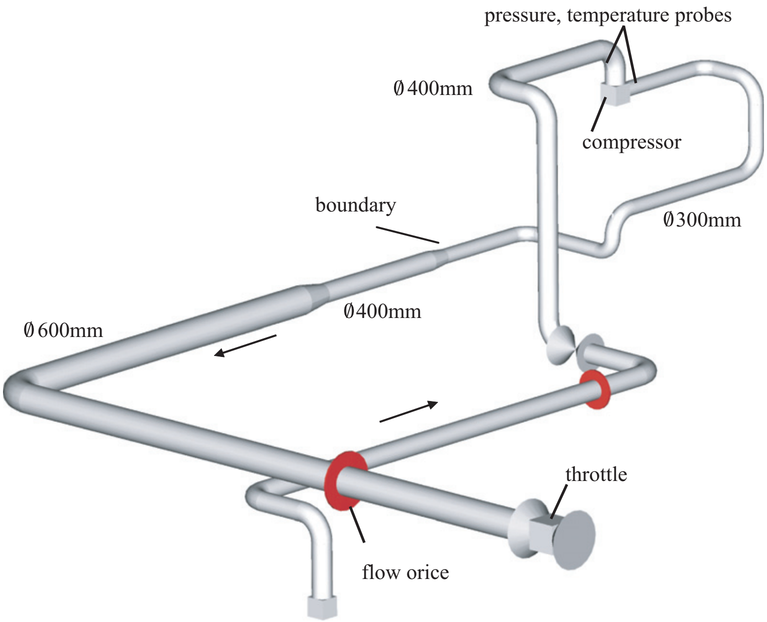

Fig. 13. Piping layout of the centrifugal compressor test rig.

Table 2
Simulation parameters of the combined Greitzer-pipeline model

Parameter	Value	Unit
Pipeline length L_p	15.4	m
Pipeline area A_p	0.0707	m^2
Plenum volume V_2	7.62	m^3
Pipe resistance R	0.674	kg/m^3s
Numerical constant κ	1.25	m^3

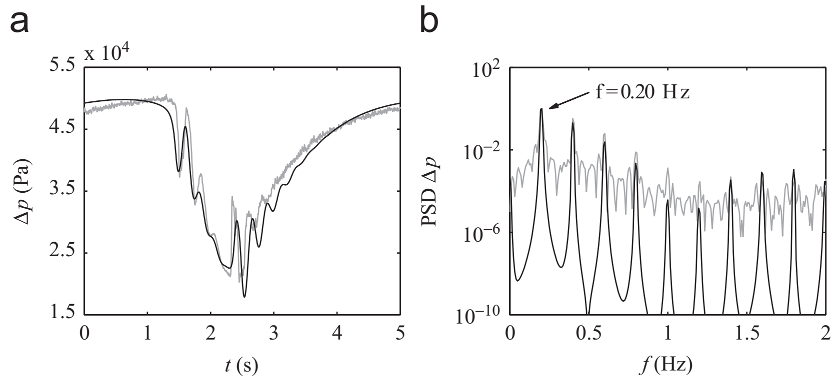

Fig. 14. Pressure measurement (gray) and simulation result after tuning of the combined Greitzer-pipeline model (black) at $N = 15,723\,\text{rev/min}$ and $\omega_l = 2/\tau$: (a) time-series and (b) power spectral density.

Afterwards we validated the obtained parameters by comparing simulation results with different sets of measurement data.

Before presenting the simulation results we will also discuss the assumption that the pipeline dynamics can be described by a linear model. The linearity assumption is justified when acoustic perturbations $\tilde{p}$, $\tilde{T}$, $\tilde{\rho}$, and $\tilde{c}$ are small compared to their undisturbed values p_0, T_0, ρ_0, and c_0. Measurement data indicates that $\tilde{p}/p_0 \approx 0.1$, $\tilde{\rho}/\rho_0 \approx 0.1$, $\tilde{T}/T_0 \approx 0.02$, and $\tilde{c}/c_0 \approx 0.02$. Furthermore, we remark that the cut-off frequency of a round pipe $\omega_{\text{cut}} = 1.84c/r$ with radius $r = 0.3\,\text{m}$ is well above the surge frequencies encountered in the compression system under study. Hence, the linearity assumption for the pipeline model is valid for all operating conditions of the compression system under study.

The simulation results for two specific measurements are shown in Figs. 14 and 15. These results show that the pipeline model extension has introduced the necessary dynamics to describe the observed pressure transients after flow reversals that arise when the compression system operates in surge. The contribution of the pipeline model extension also becomes clear from Figs. 16 and 17. From these figures we see that the extended model, in contrast to the original Greitzer model, also describes the signal components around 4 Hz that are associated with traveling waves in the discharge piping.

The period time of the transients is captured well by the extended model, although numerical tests learned that precise tuning of the model is required to predict the correct frequency of the slow surge oscillations and pipe system pulsations. In particular, the values for L_p and V_2 appear to have a large influence on the frequency of the various oscillations and transients. However, a full sensitivity analysis has not been performed so possibly there exist other (combinations of) parameters that influence the accuracy of the model predictions.

In Figs. 14 and 15, we observe that the amplitudes of the pipeline transients are predicted by the extended model with limited accuracy. Both at 15,723 and 19,512 rev/min the measured transients during back-flow (between 1 and 2 s) have a larger amplitude than the simulated ones, see Figs. 14 and 15. Furthermore, at 19,512 rev/min the damping is clearly too low during the positive flow phase of the surge cycle.

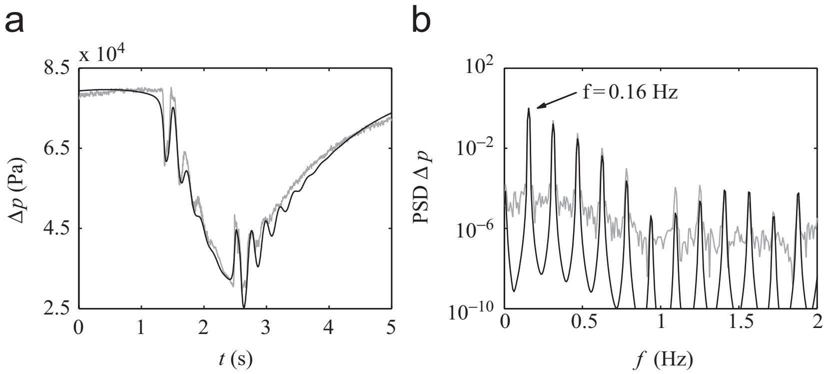

Fig. 15. Pressure measurement (gray) and simulation result after tuning of the combined Greitzer-pipeline model (black) at $N = 19,512\,\mathrm{rev/min}$ and $\omega_l = 2/\tau$: (a) time-series and (b) power spectral density.

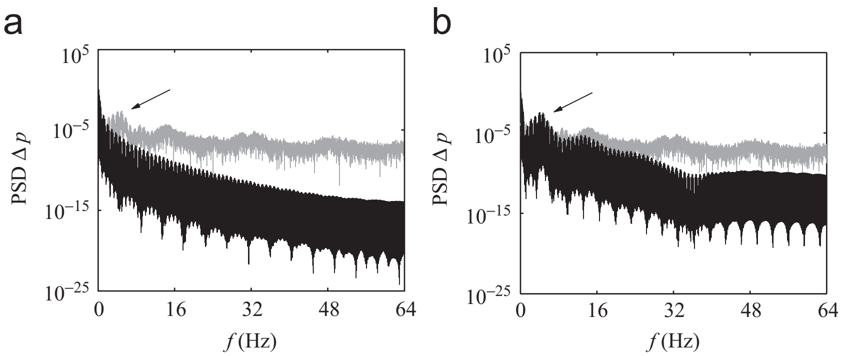

Fig. 16. Power spectral densities of measurement (gray) and simulation result (black) of the original and extended models at $N = 19,512\,\mathrm{rev/min}$ and $\omega_l = 2/\tau$: (a) Greitzer model and (b) Greitzer-pipeline model.

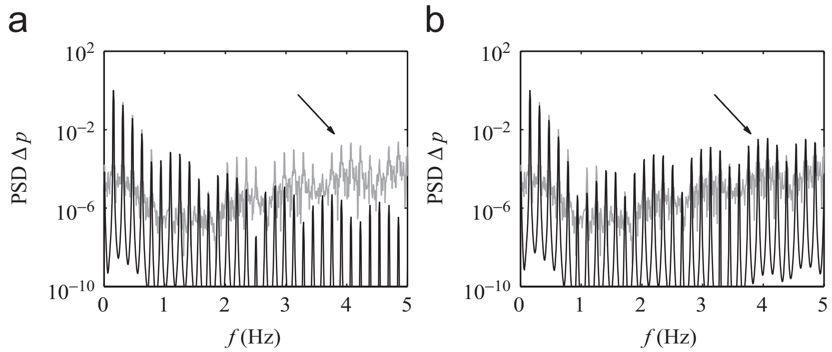

Fig. 17. Close-up of power spectral densities in region of interest of measurement (gray) and simulation result (black) of the original and extended models at $N = 19,512\,\mathrm{rev/min}$ and $\omega_l = 2/\tau$: (a) Greitzer model and (b) Greitzer-pipeline model.

By comparing Figs. 14(a) and 15(a) with Fig. 7 we see that damping of the transients appears to depend on the momentary pressure and flow velocity in the pipeline. The dependency of acoustic damping on flow conditions (density) was already mentioned in Ref. [32]. Given the above observations we modified the pipeline model by making the density ρ_0 and speed of sound c_0 a function of the momentary pressure $p_c(t)$.

This modification also caused the related model parameters (R, τ, Z_0, ω_n, ω_d, and ω_l) to become a function of $p_c(t)$.

Simulations with this modified model showed some improvements in the damping properties of the model in comparison with experimental data. However, a mismatch between the damping of measured and simulated transients remained.

The model parameter that directly influences the damping is the cut-off frequency ω_l. Hence, we made another modification to the pipeline model by applying two different values for ω_l during the periods of negative (low velocity) and positive (high velocity) flow. The values for ω_l were determined by manual tuning and we used a relay to switch between the two values. The switching behavior is illustrated in Fig. 18, showing the switching instants and the corresponding values for ω_l.

The results from the simulations with the modified pipeline model are shown in Figs. 19 and 20. We point out that including the pressure dependency of the model parameters and the switching law for ω_l, has made the pipeline model highly nonlinear.

When comparing Fig. 19 with Fig. 14 we observe that the nonlinear pipeline model has resulted in a slightly better match between the measurement and simulation. However, despite the introduced pressure dependency and the fact that damping is altered via the selection of two different values for ω_l, the amplitudes of the simulated pressure transients during back-flow are still too low. A possible explanation for this mismatch is that the effect of rotor speed variations is not captured in the model for the compression system. In a variable speed system the compressor characteristic is a function of rotor speed and this will influence the pressure and mass flow transients during surge, see for example Refs. [7,8].

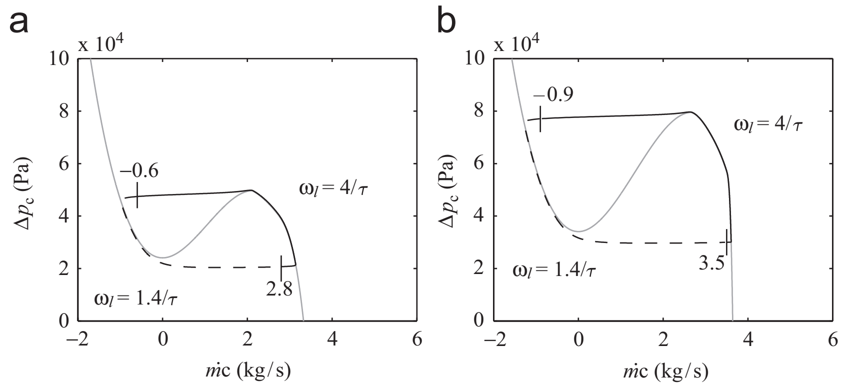

Fig. 18. Modeled switching behavior to select the value of cut-off frequency ω_l: (a) $N = 15,723$ rev/min and (b) $N = 19,512$ rev/min.

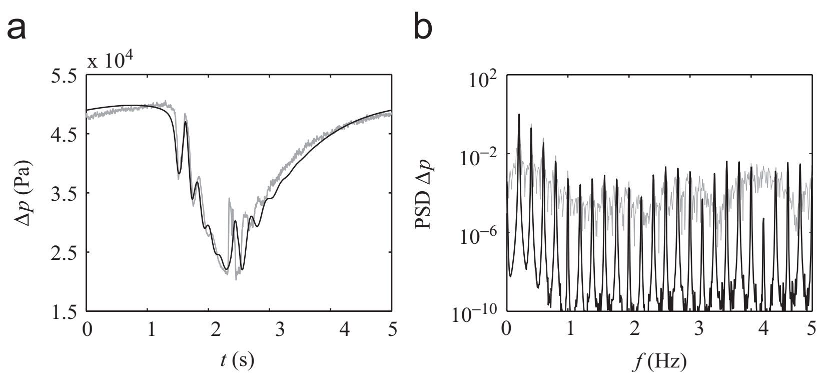

Fig. 19. Pressure measurement (gray) and simulation result after tuning of the combined Greitzer-pipeline model with velocity-dependent damping (black) at $N = 15,723$ rev/min and $\omega_l = \{1.4/\tau, 4/\tau\}$: (a) time-series and (b) power spectral density.

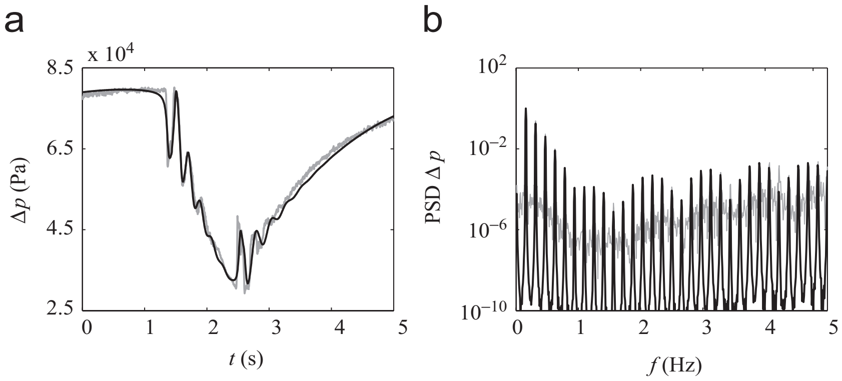

Fig. 20. Pressure measurement (gray) and simulation result after tuning of the combined Greitzer-pipeline model with velocity-dependent damping (black) at $N = 19,512\,\text{rev/min}$ and $\omega_l = \{1.4/\tau, 4/\tau\}$: (a) time-series and (b) power spectral density.

Other possible explanations for the observed differences between measurements and simulations are that the selected value for ω_l is incorrect or the simple switching method is not capable of describing the variations in acoustic damping that occur during back-flow. Furthermore, the mismatch can be caused by the inadequate modeling of friction elements like piping bends or by inaccuracies in the estimated part of the compressor curve.

For the experiment at $N = 19,512\,\text{rev/min}$ the modified model resulted in a larger improvement as can be seen in Fig. 20. The amplitudes of the acoustic transients are accurately described by the modified pipeline model. However, since the cut-off frequency in the positive flow phase is relatively low (31.7 Hz), the simulated signal starts to lag behind the measured signal due to the phase shift introduced by the low-pass filter.

5. Conclusions

In this paper, we have discussed the modeling of the dynamic behavior of large centrifugal compression systems. We applied the well-known Greitzer lumped parameter model to describe surge transients of a centrifugal compressor test rig. Comparison with experimental data showed that, after tuning the appropriate parameters, this model qualitatively and quantitatively describes the surge oscillations that occur at low mass flows with reasonable accuracy.

However, we have argued that the dynamics of a long pipe system can have a profound influence on the shape of the surge oscillations in a compression system. Experimental evidence is presented for the presence of acoustic waves in the discharge piping of the centrifugal compression system under study. The amplitude and frequency of these pipe system transients are such that a detailed study of their effect on the overall system dynamics is justified.

The main contribution of this paper is the developed aero-acoustic model for a compressor discharge line that enables the study of pipe system transients in more detail. The first benefit of the proposed model is its relative simplicity while it describes the relevant acoustic phenomena in a pipeline. We made it plausible that the assumption on which the pipeline model is based, holds for all encountered operating conditions. Secondly, the modular port–structure of the model enables a direct coupling to the dynamic Greitzer model. The good agreement between simulation results and actual surge measurements indicates that the developed model indeed captures the essential dynamics of both the compressor and the pipe system.

However, the introduced transfer function approximations contain various parameters that require tuning when the model is applied to a specific compression system. Despite the qualitatively good results that were obtained with the applied tuning approach, it seems worthwhile to investigate how these model parameters can be determined in a more structured manner, for example via experimental identification methods. In this context, it is also relevant to investigate which model parameters are critical for the accuracy of the overall model and how their uncertainty can be sufficiently reduced.

Furthermore, we argued that the quality of the resulting model critically depends on the proper selection of boundary conditions. In this paper, a rather pragmatic approach was used to select appropriate boundary conditions, partially depending on engineering experience. A more systematic approach for the correct coupling of a pipeline model to a lumped parameter compressor model will increase the applicability of the proposed model structure to other compression systems.

Finally, the validation results indicate that damping of pipe system transients depends on the local flow conditions in the pipeline. For that reason we made the model parameters a function of the momentary pressure $p_c(t)$. Furthermore, we introduced a relay nonlinearity in the model to switch between two different cut-off frequencies of a low-pass filter, effectively changing the attenuation of acoustic transients. With this relatively simple modification of the pipeline model the damping was improved. However, the obtained results illustrated that the transfer function approximations in the pipeline model are not really suited to capture all damping effects of acoustic transients during surge. More research is required in order to develop a dynamic model that adequately describes all acoustic effects in full-scale compression systems. In particular the effect of rotor speed variations on system dynamics in general and acoustic transients in particular deserves further attention.

References

[1] J. Longley, A review of nonsteady models for compressor stability, *ASME Journal of Turbomachinery* 116 (1994) 202–215.

[2] J.T. Gravdahl, O. Egeland, *Compressor Surge and Rotating Stall: Modeling and Control*, Springer, London, 1999.

[3] J.D. Paduano, E.M. Greitzer, A.H. Epstein, Compression system stability and active control, *Annual Review of Fluid Mechanics* 33 (2001) 491–517.

[4] E.M. Greitzer, Surge and rotating stall in axial flow compressors: part I—theoretical compression system model, *ASME Journal of Engineering for Power* 98 (1976) 190–198.

[5] H.W. Emmons, C.E. Paerson, H.P. Grant, Compressor surge and stall propagation, *Transactions of the ASME* 77 (1955) 455–469.

[6] K.E. Hansen, P. Jørgensen, P.S. Larsen, Experimental and theoretical study of surge in a small centrifugal compressor, *ASME Journal of Fluids Engineering* 103 (1981) 391–395.

[7] D.A. Fink, N.A. Cumpsty, E.M. Greitzer, Surge dynamics in a free-spool centrifugal compressor system, *ASME Journal of Turbomachinery* 114 (1992) 321–332.

[8] J.T. Gravdahl, O. Egeland, Centrifugal compressor surge and speed control, *IEEE Journal of Control Systems Technology* 7 (1999) 567–579.

[9] C.H.J. Meuleman, Measurement and Unsteady Flow Modelling of Centrifugal Compressor Surge, PhD Thesis, Technische Universiteit Eindhoven, Eindhoven, The Netherlands, 2002.

[10] C.R. Sparks, On the transient interaction of centrifugal compressors and their piping system, *ASME Journal of Engineering for Power* 105 (1983) 891–901.

[11] A.M. Cargill, C. Freeman, High-speed compressor surge with application to active control, *ASME Journal of Turbomachinery* 113 (1991) 303–311.

[12] M.R. Feulner, G.J. Hendricks, J.D. Paduano, Modeling for control of rotating stall in high-speed multistage axial compressors, *ASME Journal of Turbomachinery* 118 (1996) 1–10.

[13] W.M. Jungowski, M.H. Weiss, G.R. Price, Pressure oscillations occurring in a centrifugal compressor system with and without passive and active surge control, *ASME Journal of Turbomachinery* 118 (1996) 29–40.

[14] A. Eijk, G. Egas, J.P.M. Smeulers, Cost-effective and detailed modelling of compressor manifold vibrations, *Proceedings of the ASME Pressure Vessels and Conference*, Montreal, Canada, 1996, pp. 415–425.

[15] A. Eijk, G. Egas, Effective combination of on-site measurements and simulations for a reciprocating compressor system, *Proceedings of the Second EFRC Symposium*, The Hague, The Netherlands, 2001.

[16] G. Egas, PULSIM, a powerful tool to prevent vibrations in pipe systems', *Proceedings of the First European Forum on Materials and Products for Noise and Vibration Control in Machinery and Transportation*, Senlis, France, 2001.

[17] R.E. Goodson, R.G. Leonard, A survey of modeling techniques for fluid line transients, *ASME Journal of Basic Engineering* 94 (1972) 474–482.

[18] J.S. Stecki, D.C. Davis, Fluid transmission lines—distributed parameter models, part 1: a review of the state of the art, *Proceedings of the IMechE* 200 (1986) 215–228.

[19] M.J. Munjal, *Acoustics of Ducts and Mufflers*, Wiley-Interscience, Chichester, 1987.

[20] M.S. Howe, *Acoustics of Fluid–Structure Interactions*, Cambridge University Press, Cambridge, 1998.

[21] L.E. Kinsler, A.R. Frey, A.B. Coppens, J.V. Sanders, *Fundamentals of Acoustics*, fourth ed., Wiley, New York, 1999.

[22] ISO International Standard, part 2: orifice plates, *Measurement of Fluid Flow by Means of Pressure Differential Devices Inserted in Circular-Cross-section Conduits Running Full*, second ed., no. 5167-2:2003(E), International Organization for Standardization, Geneva, 2003.

[23] F.P.T. Willems, Modeling and Bounded Feedback Stabilization of Centrifugal Compressor Surge, PhD Thesis, Technische Universiteit Eindhoven, Eindhoven, The Netherlands, 2000.
[24] IEC International Standard, part 2-1: flow capacity—sizing equations for fluid flow under installed conditions, *Industrial-Process Control Valves*, first ed., no. 60534-2-1, International Electrotechnical Commission, Geneva, 1989.
[25] J. v. Helvoirt, B. d. Jager, M. Steinbuch, J. Smeulers, Stability parameter identification for a centrifugal compression system, *Proceedings of the 43rd IEEE Conference on Decision and Control*, Atlantis, Paradise Island, Bahamas, 2004, pp. 3400–3405.
[26] J. v. Helvoirt, B. d. Jager, M. Steinbuch, J. Smeulers, Modeling and identification of centrifugal compressor dynamics with approximate realizations, *Proceedings of the 2005 IEEE Conference Control Applications*, Toronto, Canada, 2005, pp. 1441–1447.
[27] A. Hirschberg, J. Kergomard, G. Weinreich (Eds.), *Mechanics of Musical Instruments*, *CISM Courses and Lectures*, Vol. 355, Springer, Wien, 1995.
[28] F. Albertson, H. Bodén, J. Gilbert, Comparison of different methods to couple nonlinear source descriptions in the time domain to linear system descriptions in the frequency domain—application to a simple valveless one-cylinder cold engine, *Journal of Sound and Vibration* 291 (2006) 963–985.
[29] R.E. Matick, *Transmission Lines for Digital and Communication Networks*, IEEE Press, Piscataway, 1995.
[30] J.O.I. Smith, Physical modeling using digital waveguides, *Computer Music Journal* 16 (1992) 74–91 (special issue on Physical Modeling of Musical Instruments, Part I).
[31] P. Krus, K. Weddfelt, J. Palmberg, Fast pipeline models for simulation of hydraulic systems, *ASME Journal of Dynamic Systems, Measurements, and Control* 116 (1994) 132–136.
[32] S.A. Whitmore, T.R. Moes, The effects of pressure sensor acoustics on airdata derived from a high-angle-of-attack flush airdata sensing (HI-FADS) system, Technical Report TM-101736, NASA, 1991.
[33] W.C. Yang, W.E. Tobler, Dissipative model approximation of fluid transmission lines using linear friction model, *ASME Journal of Dynamic Systems, Measurements, and Control* 113 (1991) 152–162.
[34] S.A. Whitmore, Formulation of a general technique for predicting pneumatic attenuation errors in airborne pressure sensing devices, Technical Report TM-100430, NASA, 1988.
[35] H.D. Baehr, K. Schwier, *Die Thermodynamischen Eigenschaften der Luft*, Springer, Berlin, 1961.